International Journal of Science and Research (IJSR)
ISSN (Online): 2319-7064
Impact Factor (2012): 3.358

Bio Synthesis and Characterisation of Fe_3O_4 Nanoparticles Using Caricaya Papaya Leaves Extract

N. Latha[1], M. Gowri[2]

PG & Research Department of Chemistry, Kandaswami Kandar's College, Paramathi Velur, Tamilnadu, India

Abstract: ***Fe_3O_4 nanoparticles were prepared by using caricaya papaya leaves extract at room temperature. The synthesized nanoparticles were characterised by using UV-Vis absorption spectroscopy, FT-IR, XRD, SEM with EDS techniques. UV-Vis absorption shows a characteristic absorption peak of iron oxide nanoparticles in the range of 190-250 nm. FT-IR measurement was carried out to identify the possible molecules like carbonyl, CH, OH band. From the XRD, it was found that the average particle size of magnetite nanoparticles was found to be 33 nm. SEM shows the plate like structure with coarsened grains and capsule like morphology and EDS showed its chemical composition. This biosynthesis approach is cost effective, eco-friendly and promising for applications in medicine.***

Keywords: Biosynthesis, Ferric chloride, Caricaya papaya leaves, Ironoxide nanoparticles.

1. Introduction

Biosynthesis of metal nanoparticles from plant systems is an emerging as a new and recent development technique. The nanoparticles are of great interest due to their extremely small size and large surface to volume ratio, and they exhibited utterly novel characteristics compared to the large particles of bulk material. There is increasing in commercial demand for nanoparticles due to their wide applicability in various areas such as energy, electronics, catalysis, chemistry and medicine. Recently, an extensive research has been focussed on nano-structured magnetite because it posses unique magnetic and electric properties and its application in medical treatment [1-8].

Nanoparticles are traditionally synthesised by wet chemical techniques, where the chemical used are quite often toxic and flammable. A conventional method to prepare the iron oxide nanoparticles are coprecipitation method [9-11]. A number of approaches are available for the synthesis of iron oxide nanoparticles such as attrition, top-down method, bottom-up method, sonochemical process, hydrodynamic cavitation, microemulsion process, radiolysis, microwave, laser ablation method and recently via the biosynthesis route [12-17].

The synthesis of metal nanoparticles using inactivated plant tissue, plant extract [18], exudates [19] and other parts of living plants is a modern alternative for their production. The stable iron oxide nanoparticle synthesized from plants towards green principle approach is a novel method to overcome the limitation of other conventional methods. The main advantage of this method is its ability to control the size and shape of nanoparticle and its properties. In this green synthesis route, the bio-molecules in plants can act as capping and reducing agents and thus increases the rate of reduction and stabilization of nanoparticles.

The Fe_3O_4 nanoparticles have synthesized from various plants have different applications in various sectors [20]. Particularly a few report have been studied the caricaya papaya leaves Extract was used to synthesise different metal nanoparticles [21] except Fe_3O_4. In the present study deals with biosynthesis and characterization of stable Fe_3O_4 nanoparticles from caricaya papaya leaves Extract.

2. Materials and Methods

2.1 Materials

Ferric chloride hexahydrate ($FeCl_3.6H_2O$, AR), was purchased from Merck without purification. Solutions prepared from double distilled water.

2.2 Preparation of caricaya papaya leaves Extract

About 20-25g of fresh leaves of Caricaya papayas were thoroughly washed with distilled water and cut into small pieces then heated at 70^0C in 250 ml glass beaker along with 100 ml of double distilled water for 15 minutes. After boiling, the colour of the aqueous solution changed from watery to brown colour and allowed to cool to room temperature. The aqueous extract of caricaya papaya was separated by filtration with Whatman No.42 filter paper.

2.3 Synthesis of Fe_3O_4 Nanoparticles

Various concentration of metal ions (0.01M, 0.02M, 0.1M, 0.2M) solutions were mixed with different volume (2, 4, 6, 8, 10 ml) of the caricaya papaya leaves extract. After few minutes depending on the concentration of metal ions and volume of the extract, the colour of the solution changed from brown to black indicating the formation of iron oxides nanoparticles (Fig.1.). The solid product was filtered and washed with ethanol and then dried at room temperature.

2.4 Characterization

UV-Vis spectroscopic studies were carried out caricaya papaya extract and metal nanoparticles using a Lambda 35 (Make, Perkin Elemer) double beam spectrophotometer in the range of 190 nm-1100 nm. FT-IR spectra of caricaya

papaya extract and metal nanoparticles were done by using FT-IR spectrophotometer (Model RXI, Make Perkin Elemer) in the range of 4000 - 400 cm^{-1} using KBr pellet method. The morphology of synthesized iron oxide nanoparticles and elemental analysis was examined by Scanning Electron Microscopy (SEM), (Model TESCAN VEGA 3 LMU -USA) equipped with energy dispersive spectrum (EDS), (BRUCKER NANO GMBH - GERMANY). Fe_3O_4 nanoparticles synthesised by this bio-route were recorded with Philips analytical X-Ray Diffractometer using CuKα radiation source operated at 40 KV and 30 MA.

3. Results and Discussion

The addition of Ferric chloride solution to the Caricaya papaya leaves extract the reduction reaction takes place of Fe^{3+} to Fe_3O_4. A possible reaction beyond the formation of iron oxide nanoparticles is Ferric chloride ($FeCl_3 .6H_2O$) and caricaya papaya leaf extract are involved in the reaction of aqueous phase medium. Initially, the C=O of aldehyde group in caricaya papaya leaf extract chelated with Fe^{3+} ions to form ferric protein chains HO^-.... Fe^{3+}..... bonds and as result in the formation of suspended ferric hydroxide $Fe(OH)_3$. Subsequently on slow evaporation, ferric hydroxide in a core is dehydrated ($-H_2O$) to form a black coloured magnetite (Fe_3O_4) nanoparticle as a crystals. The protein chain in a caricaya papaya leaf extract covered on Fe_3O_4 surface through chelation of COO^- .....Fe^{3+}.

3.1 UV –Vis spectral analysis

Formation and stability of iron oxide nanoparticles in aqueous colloidal solution is confirmed by using UV-Vis spectral analysis. 2, 4, 6, 8, 10 mL of caricaya papaya leaves extract were mixed with 15 mL of 0.01 M, 0.02 M, 0.1 M, 0.2 M of aqueous solution of ferric chloride solution resulted in colour change of the solution from brown to black due to formation of ironoxide nanoparticles. The colour changes arise from the excitation of the surface plasman resonance (SPR) phenomenon typically of iron oxide nanoparticles [22]. The optical absorption spectrum of metal nanoparticles depends on the particle size, shape, state of aggregation and the surrounding dielectric medium [23]. The appearance of black colour indicates the formation of iron oxide nanoparticles.

Caricaya papaya leaves extract has the absorption peaks at the wavelength of 204 nm and intensity of absorption is 2.9 is represented in Fig.2. Ferrric chloride has the absorption peaks at the wavelength of 241 nm and the intensity of absorption is 4.1 is shown in Fig.3. Fig.4-7. shows the UV-Vis spectra of iron oxide nanoparticles formed from 0.01 M, 0.02 M, 0.1 M and 0.2 M of $FeCl_3$ solution with 2, 4, 6, 8, 10 mL of plant extract. Increase in metal ion concentration with constant volume of plant extract, increase in wavelength of absorption due to the higher production of nanoparticles. It was observed that the intensity of absorbance steadily increases with increase in metal ion concentration and reaches maximum 5.3 after that the values decreases.

The characteristic surface plasmon resonance band of Fe_3O_4 occurs at wavelength in the range of 190-250 nm as a function of different concentration of metal ion with different volume of plant extracts at room temperature. The maximum SPR band centered at 248 nm, which indicates the reduction of $FeCl_3$ into Fe_3O_4.

3.2 FT-IR Spectroscopy

FT-IR analysis was performed, in order to determine the functional groups on papaya leaves extract and predict their role in the synthesis of iron oxide nanoparticles. Fig.8 shows the FT-IR spectrum of papaya leaf extract. The strong absorption peak at 3434 cm^{-1} is assigned to O-H stretching of alcohol and phenolic compounds or stretching of the –NH band of amino group. The presence of peak at 2398 and 2082 cm^{-1} are assigned to aliphatic C-H stretching in methyl and methylene groups [24]. The peak at 1635 cm^{-1} is due to stretching vibration of CO groups in the ketones, aldehydes and carboxylic acids. The peak belonging to 1437 cm^{-1} is due to COO stretching vibration [25]. The peak at 661cm^{-1} is due to finger print region and it difficult to assign single functional groups.

FT-IR spectrum of synthesized Fe_3O_4 nanoparticles using papaya leaf extracts is presented in Fig.9. The following bands were observed. Peaks at 3393 cm^{-1} is assigned to the OH stretching of alcohol and phenol [26]. Signals at 2931 cm^{-1} indicate the presence of CH stretching groups. The absorption peak at 1659 cm^{-1} may be assigned to the amide band of proteins arising from carbonyl stretching in proteins. The peak at 1412 cm^{-1} is attributed to the presence of carboxylate ions (COO^-), which is responsible for the formation of iron oxide nanoparticles. The peaks at 1064 and 1325 cm^{-1} indicate the presence of CO groups [27]. The formation of Fe_3O_4 is characterised by the absorption bands from 418 to 502 cm^{-1} is corresponds to the Fe–O band [28]. This peak was absent in plant extract which indicate the formation of iron oxide nanoparticles. The absorbance band at 617 cm^{-1} might be assigned to the existence of some amount of oxidised iron oxide on the surface. FT-IR analysis confirmed that the bioreduction of ferric chloride into iron oxide nanoparticles are due to the reduction by capping material of caricaya papaya leaf extract.

3.3 Scanning Electron Microscopy analysis

A scanning electron microscopy was employed to analyse the structure of nanoparticles that were formed. Fig.10. (a, b) shows the low magnification (2.55 kx, 4.22 kx) SEM image of Fe_3O_4 powder; it can be seen that the particles are agglomerated. The size distribution and morphology is irregular. The particles are plate like structure with coarsened grains, whereas the magnification at 8.00 kx in Fig.10.(c), the Fe_3O_4 nanoparticles showed uniformly distributed small spherical shaped particles. The magnification at 10.44 kx Fig.10.(d) under the same conditions, which showed that large number of homogeneous nanocapsule like morphology of iron oxide nanoparticles.

3.4 Energy Dispersive Spectroscopic Analysis

EDS analysis was carried out to determine the elemental composition and stoichiometry of the synthesized iron oxide nanoparticles, which is presented in Fig.11. Iron, oxygen signals and other signals also have been detected. The other signal may be coming from the bio active molecules in the Caricaya papaya leaves extract. It implies that the nanoparticles are mainly indeed made up of only Fe and O [29]. Therefore the magnetite nanoparticles were successfully synthesised by this green method using caricaya papaya leaves extract as stabilizer for nanoparticles

3.5 XRD Analysis

XRD is an effective characterization to confirm the crystal structure of the synthesised magnetite nanoparticles. Fig. 12 shows the XRD patterns of the iron oxide nanoparticle. Peaks at 2θ =29.11^o, 41.26^o, 51.8^o, 67.67^o and 74.44^o are attributed to magnetite Fe_3O_4 (0 2 2), (1 2 2), (0 2 5), (2 1 0) and (2 3 0) planes, respectively. Clearly, all the peaks in the patterns are consistent with the values of the standard JCPDS values (File no. 89-6466, a=2.7992, b=9.4097, c=9.4832) can be indexed to pure Fe_3O_4 with Orthorhombic structure. No peaks due to impurities were detected. Crystal size of the synthesized nanoparticles was calculated from the Debye-Scherrer equation $D = K\lambda / \beta \cos\theta$ [30]. Where D is the crystallite size of iron oxide nanoparticles, λ is the wavelength of the X –ray source (0.1541 nm), β is the full width at half maximium of the diffraction peak, K is the Scherrer constant with a value of 0.9, and θ is the half diffraction angle - Bragg angle. The average crystals size of the iron oxide nanoparticle was found to be 33 nm. XRD pattern reveals that the iron oxide nanoparticles prepared by bio-route method are crystalline [31].

3. Conclusions

Synthesis of iron oxide nanoparticles was quite stable without using any toxic chemicals as capping agents. Colour changes arises due to the surface plasmon resonance during the reaction with the ingredients presents in the caricaya papaya leaves extract resulting in the formation of iron oxide nanoparticles, which is confirmed by UV-Vis spectroscopy, FT-IR, SEM with EDS analysis. From the XRD analysis the average crystal of iron oxide nanoparticles was found to be 33 nm. In this approach is highly promising for the green, sustainable production of magnetite nanoparticles.

References

[1] J. Kim, J. E. Lee, J. Lee, J. H. Yu, B. C. Kim, K. An, Y. Hwang, C. H. Shin, J.G. Park, J. Kim and T. Hyeon , J. Amer. Chem. Soc., 128, 688 **(2006)**.
[2] Y. W. Jun, Y. M. Huh, J. S. Choi, J. H. Lee, H. T. Song, S. Kim, S. Kim, S. Yoon, K. S. Kim, J. S. Shin, J. S. Suh and J. Cheon , J. Amer. Chem. Soc., 127, 5732 **(2005).**
[3] H. T. Song, J. S. Choi, Y. M. Huh, S. Kim, Y. W.Jun, J. S. Suh and T. Cheon, J. Amer. Chem. Soc., 127, 9992 **(2005).**
[4] O. Bretcanu, E. Verne, M. Coisson, P. Tiberto and P. Allia, J. Magnetism and Magnetic Mat., 305, 529 **(2006)**.
[5] M. Johannsen, U. Gneveckow, K. Taymoorian, B. Thiesen, N. Waldofner, R. Scholz, K. Jung, A. Jordan, P. Wust and S. A. Loening, Int. J. Hyperth., 23, 315 **(2007)**.
[6] K. E. McCloskey, J. J. Chalmers and M. Zborowski, Anal. Chem., 75, 6868 **(2003).**
[7] A. K. Gupta and S. Wells, Nanobiosci., 3, 66 **(2004)**.
[8] X. Wei and R. C. Viadero, Physicochem. Aspects, 294, 280 **(2007).**
[9] S. J. Lee, J. R. Jeong, S. C. Shin, J. C. Kim and J. D. Kim, J. Magnetism and Magnetic Mat., 282, 147 **(2004).**
[10] Y. Hou, Z. Xu, and S. Sun, Angew. Chem. Int. Ed., 46, 6329 **(2007)**.
[11] D. Predoi, Dig. J. Nanomat. and Biostr., 2(1), 169 **(2007).**
[12] L. Rodriguez-Sanchez, M. C. Blanco and M. A. Lopez-Quintela, J. Phys. Chem. B., 104**,** 9683 **(2000).**
[13] J. J. Zhu, S. W. Liu, O. Palchik, Y. Koltypin and A. Gedanken, Langmuir., 16, 6396 **(2000).**
[14] Pastoriza-Santos and L. M. Liz-Marzan, Langmuir, 18, 2888 **(2002).**
[15] N. A. Begum, S. Mondal, S. Basu, R. A. Laskar and D.Mandal, Colloids and Surfaces B: Biointerfaces, 71(1), 113 **(2009).**
[16] H. Bar, D. K. Bhui, G. P. Sahoo, P. Sarkar, S. P. De and A. Misra, Physicochemical and Eng. Aspects, 339, 134 **(2009).**
[17] J. Y. Song and B. S. Kim, Bioprocess Biosyst. Eng., 32, 79 **(2009).**
[18] K. Shameli, M. B. Ahmad, A. Zamanian, P. Sangpour, P. Shabanzadeh, Y. Abdollahi and M. Zargar, Int. J. Nanomedicine., 7, 5603 (**2012).**
[19] A. I. Lukman, B. Gong, C. E. Marjo, U. Roessner and A. T. Harris, J. Colloid Interface Sci., 353, 433 (**2011).**
[20] M. Pattanayak and P. L. Nayak, Int. J. Plant, Animal and Envir. Sci. 3, 1 **(2013)**
[21] Ratika Komal and Vedpriya Arya Int. J. Nanomat. and Biostr. 3, 1 **(2013)**
[22] S. S. Shankar, A. Rai, B. Ankamwar, A. Singh, A. Ahmad and M. Sastry, Nat. Mater., 3, 482 **(2004)**.
[23] R. K. Petla, S. Vivekanandhan, M. Misra, A. K. Mohanty and N. Satyanarayana, J. Biomat. Nanobiotechnol., 3, 14 **(2012)**.
[24] R. R. R. Kannan, W. A. Stirk and J. Van Staden, S. Afr. J. Bot., 86, 1 **(2013).**
[25] S. Kaviya, J. Santhanalakshmi and B. Viswanathan, Mat. Lett., 67, 64 **(2012)**.
[26] W. Cai and J. Q. Wan, J. Colloid Interface Sci.,305, 366 **(2007).**
[27] H. Bar, D. K. Bhui, G. P. Sahoo, P. Sankar, S. P. De and A. Misra, Colloids and Surfaces A : Physicochem. Eng. Aspects, 339, 134 **(2009)**.
[28] H. R. Wang and K. M. Chen, Colloids and Surfaces A: Physicochem. Eng. Aspects., 281, 190 **(2006).**
[29] M. Noruzi, D. Zare and D. Davoodi, Spectrochim. Acta A Mol. Biomol. Spectros., 94, 84 **(2012)** .
[30] Y. Zhu and Q. Wu, J. Nanoparticle Res., 1, 393 **(1999)**
[31] C. J. Chen, H-Y Lai, C. C. Lin, J. S Wang and R. K. Chiang, Nanoscale Res. Lett., 4, 1343 **(2009)**

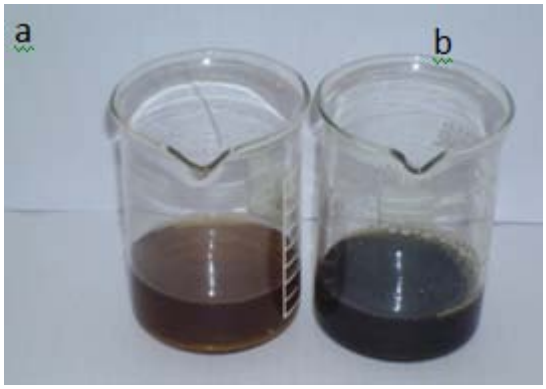

Figure 1: Papaya leaves extract (a) before; (b) after synthesis of iron oxide nanoparticles

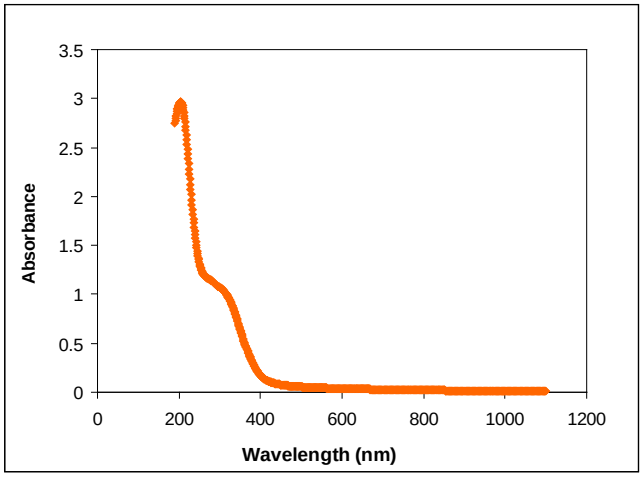

Figure 2: UV absorption spectrum of papaya leaves extract

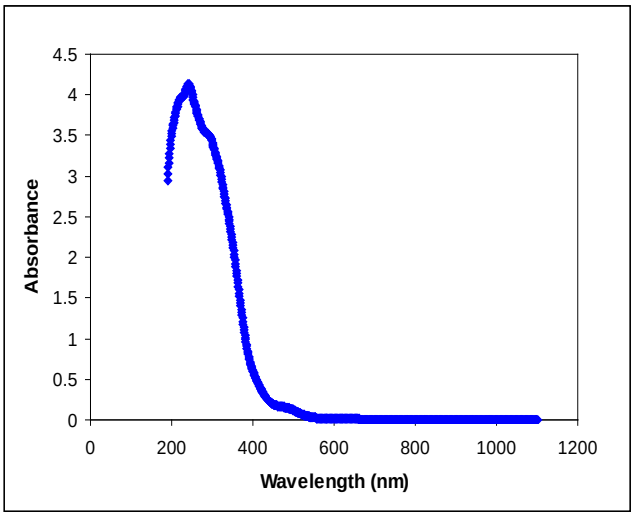

Figure 3: UV absorption spectrum of 0.2M $FeCl_3$ solution

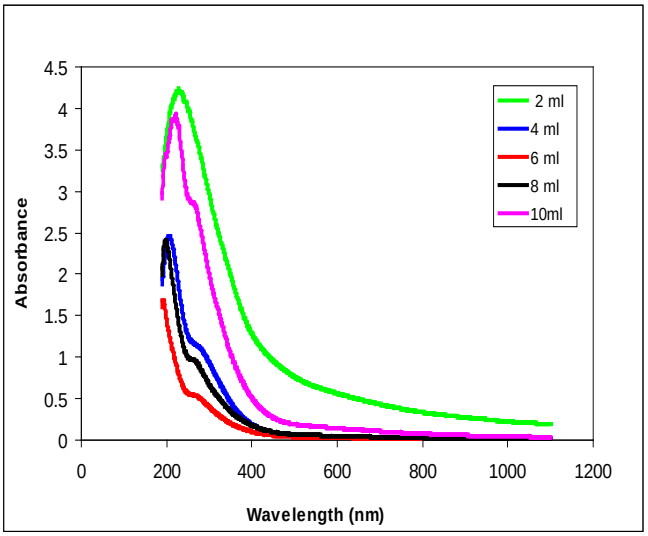

Figure 4: UV absorption spectrum of 0.01M $FeCl_3$ with different volume of plant extracts

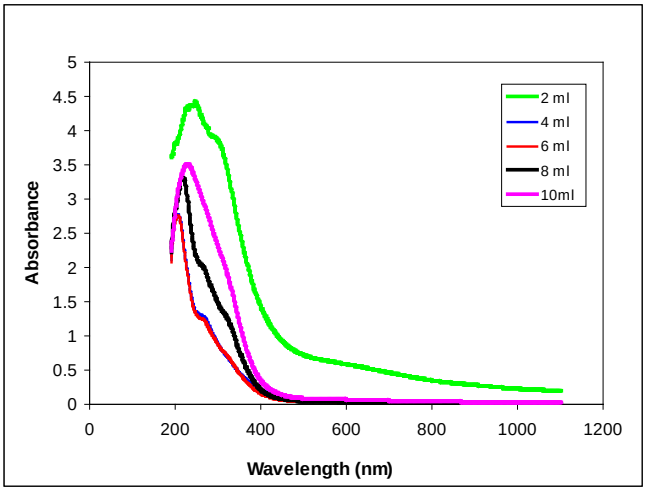

Figure 5: UV absorption spectrum of 0.02M $FeCl_3$ with different volume of plant extracts

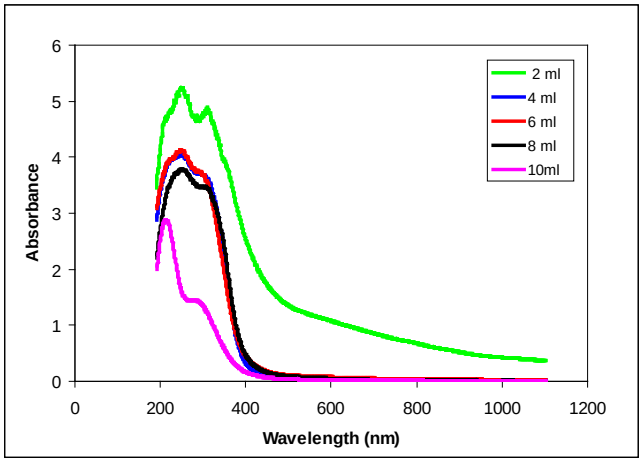

Figure 6: UV absorption spectrum of 0.1M $FeCl_3$ with different volume of plant extracts

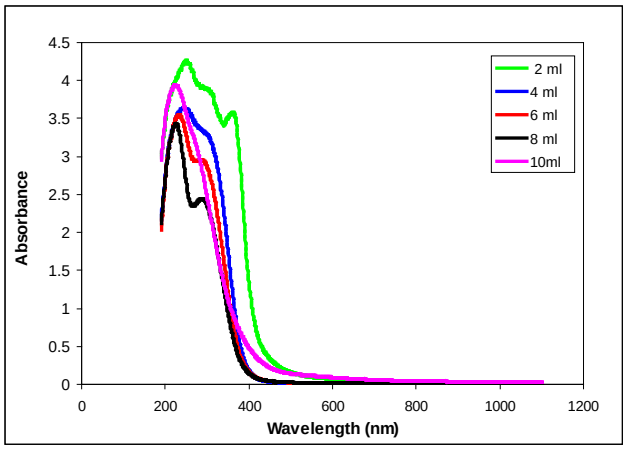

Figure 7: UV absorption spectrum of 0.2M $FeCl_3$ with different volume of plant extracts

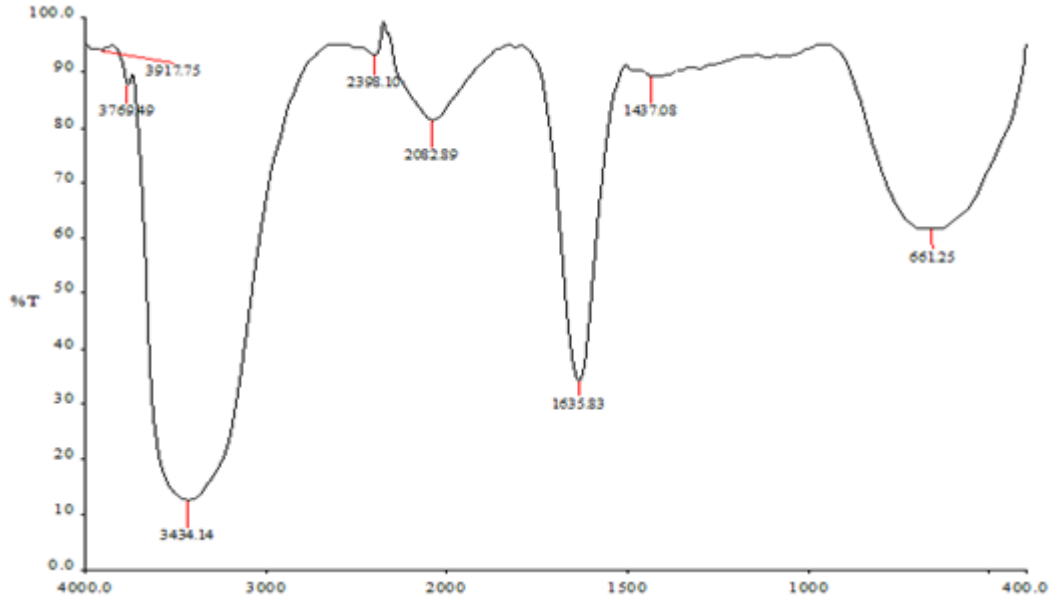

Figure 8: FT-IR spectra of caricaya papaya leaves extract

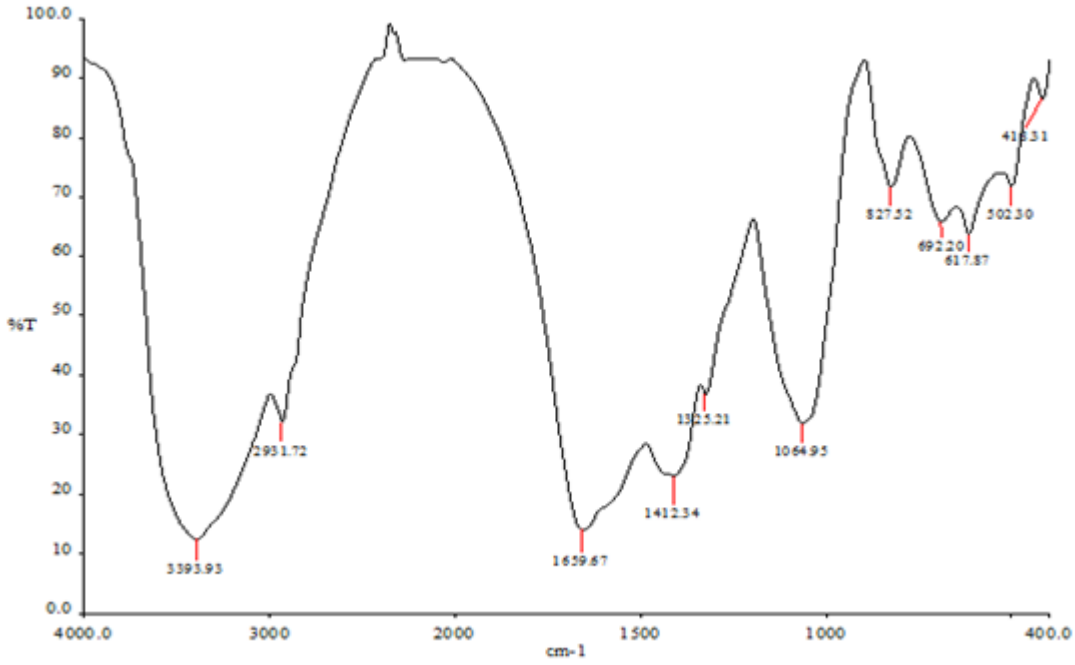

Figure 9: FT-IR spectrum of Fe_3O_4 nanoparticles using papaya leaf extract

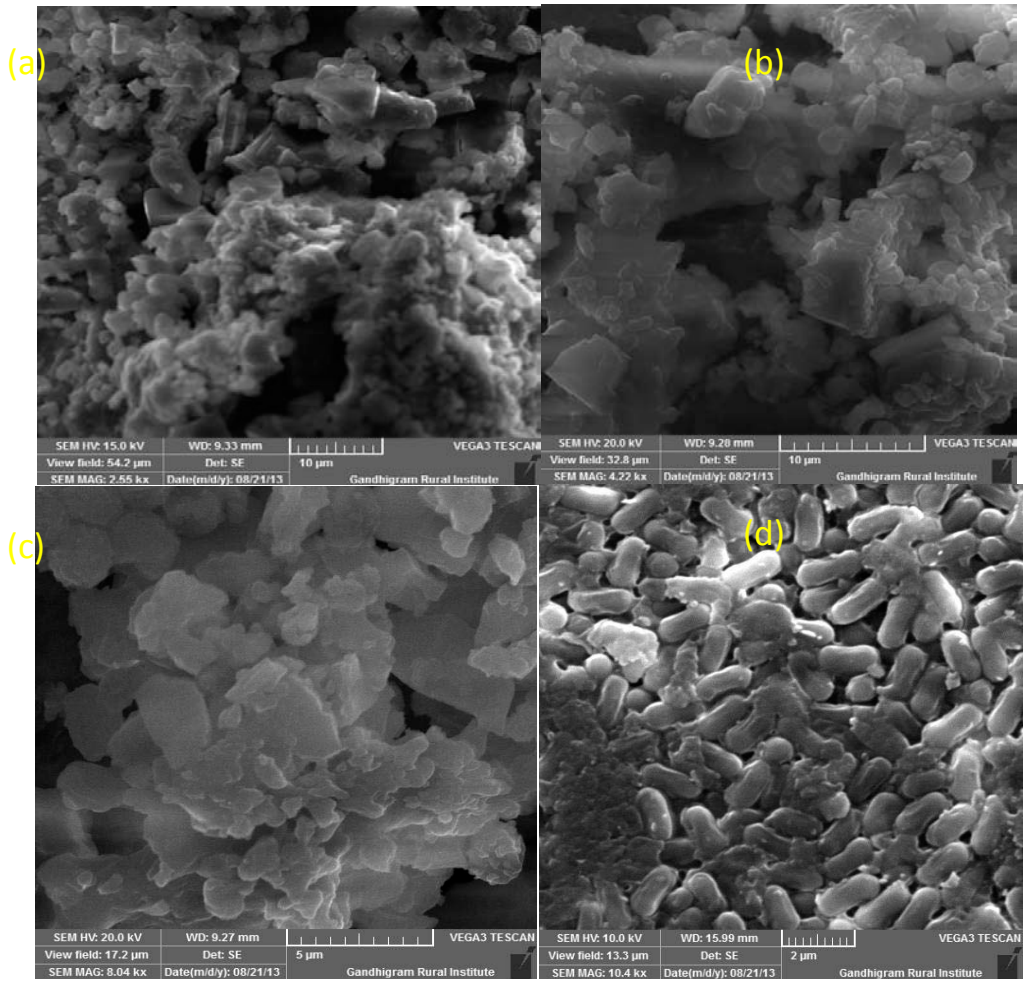

Figure 10: (a, b, c & d) SEM image of Fe_3O_4 nanoparticles synthesized using caricaya papaya leaf extract at different magnification levels

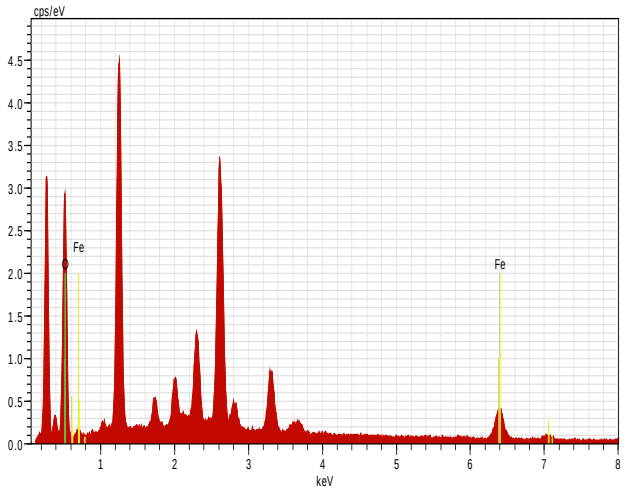

Figure 11: Energy dispersive X-ray spectra of synthesized Fe_3O_4 nanoparticles

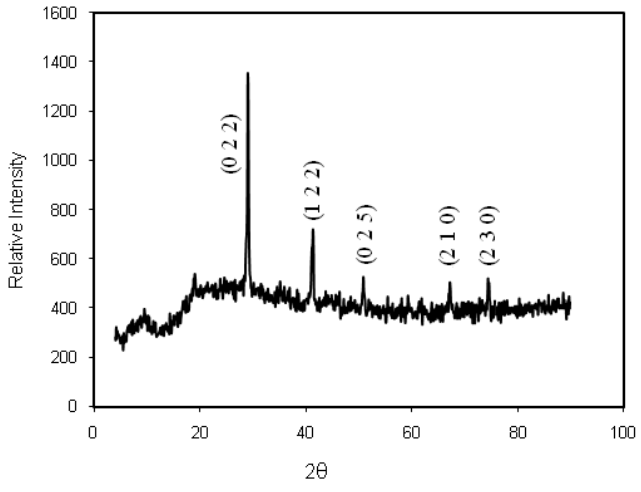

Figure 12: XRD pattern of Fe_3O_4 nanoparticles synthesised using papaya leaf extract